

# Probabilistic Scheduling of UFLS to Secure Credible Contingencies in Low Inertia Systems

Cormac O’Malley, *Student Member, IEEE*, Luis Badesa, *Member, IEEE*, Fei Teng, *Member, IEEE*, and Goran Strbac, *Member, IEEE*

**Abstract**—The reduced inertia levels in low-carbon power grids necessitate explicit constraints to limit frequency’s nadir and rate of change during scheduling. This can result in significant curtailment of renewable energy due to the minimum generation of thermal plants that are needed to provide frequency response (FR) and inertia. Additional consideration of fast FR, a dynamically reduced largest loss and under frequency load shedding (UFLS) allows frequency security to be achieved more cost effectively. This paper derives a novel nadir constraint from the swing equation that, for the first time, provides a framework for the optimal comparison of all these services. We demonstrate that this constraint can be accurately and conservatively approximated for moderate UFLS levels with a second order cone (SOC), resulting in highly tractable convex problems. Case studies performed on a Great Britain 2030 system demonstrate that UFLS as an option to contain single plant outages can reduce annual operational costs by up to £559m, 52% of frequency security costs. The sensitivity of this value to wind penetration, abundance of alternative frequency services, UFLS amount and cost is explored.

**Index Terms**—Inertia, Frequency Response, Stochastic Unit Commitment, UFLS, Wind Energy

## NOMENCLATURE

### Indices and Sets

|        |                                           |
|--------|-------------------------------------------|
| $n, N$ | Index, Set of nodes in the scenario tree. |
| $g, G$ | Index, Set of generators.                 |
| $k, K$ | Index, Set of UFLS levels.                |

### Constants

|                   |                                                          |
|-------------------|----------------------------------------------------------|
| $\pi(n)$          | Probability of reaching node $n$ .                       |
| $\Delta\tau(n)$   | Time-step corresponding to node $n$ (h).                 |
| $c_{LS}$          | Value of load-shed from lack of reserve (£/MWh).         |
| $f_0$             | Nominal grid frequency (Hz).                             |
| $\Delta f_{trig}$ | Low frequency deviation at which UFLS is triggered (Hz). |
| $P_k^{UFLS}$      | Load-shed amount at level $k$ (GW).                      |
| $t_{rec}$         | Disconnection length of UFLS (h).                        |
| $p$               | Probability of $PL_{max}$ outage (occurrences/h).        |
| $N_{PL_{max}}$    | Number of units generating at $PL_{max}$ .               |
| $T_i$             | Delivery speed of FR type $i$ (s).                       |
| $c_k^{UFLS}$      | Value of load-shed at UFLS level $k$ (£/MWh).            |
| $M$               | Big-M constant.                                          |
| $RoCoF_{max}$     | Maximum admissible RoCoF (Hz/s).                         |

### Decision Variables (continuous unless stated)

|             |                                                    |
|-------------|----------------------------------------------------|
| $P^{LS}(n)$ | Load-shed from lack of reserve at node $n$ (GW).   |
| $PL_{max}$  | Largest power infeed (GW).                         |
| $H$         | System inertia after the loss of $PL_{max}$ (GWs). |
| $R_i$       | Magnitude of type $i$ FR (GW).                     |
| $m_k$       | Binary variable corresponding to UFLS level $k$ .  |

### Linear Expressions of Decision Variables

|           |                                              |
|-----------|----------------------------------------------|
| $C_g(n)$  | Operating cost of units $g$ at node $n$ (£). |
| $C^U(n)$  | Expected cost of UFLS at node $n$ (£).       |
| $R_i(t)$  | Time evolution of FR type $i$ (GW).          |
| $X, Y, Z$ | Auxiliary expressions for eq. (10).          |

### Nonlinear Expressions of Decision Variables

|               |                                                                      |
|---------------|----------------------------------------------------------------------|
| $\Delta f(t)$ | Frequency deviation at time $t$ after outage (Hz).                   |
| $\hat{t}$     | Time after outage that frequency reaches the UFLS trigger level (s). |

## I. INTRODUCTION

GRID frequency needs to be kept within boundaries to prevent system damage and emergency demand disconnection. The rate of change of frequency (RoCoF) is determined by the instantaneous generation-demand imbalance. Post generator outage, the frequency’s evolution is dictated by the available frequency services (FS) including inertia and FR.

Synchronous thermal generators provide inertial response from the kinetic energy stored in their rotating turbines and FR from governor droop controls. Decarbonisation replaces synchronous thermal generators with renewable energy sources. This means that frequency security is no longer guaranteed by meeting energy demand alone because currently, converter based generation (like wind) is often not able or not incentivised to provide any FS. Thus explicit frequency security constraints must be included in scheduling to assure system stability. This can result in significant wind curtailment due to the minimum generation from thermal plants that are needed to provide FS [1], negatively impacting costs and emissions. The increase in operational cost is referred to here as a system’s frequency security cost (FSC).

This motivates the investigation of other possible tools at the disposal of system operators to contain the frequency more cost effectively. UFLS results in a step decrease in demand. It is used traditionally as a last resort containment measure after very large outages (non-credible/unsecured events) [2], and its potential role to support frequency control during normal operation has been overlooked.

The majority of UFLS literature focuses on how to contain unsecured events with the least load shed [3]. This necessitates a fast nadir prediction following the event, from which the optimum load to be shed can be calculated online. If the outage size is known, then the single machine swing equation can be used [4]. When outage size is unknown, it can be estimated from initial RoCoF measurements [5]. Alternatively, the future frequency evolution can be predicted directly from frequency measurements post disturbance [6]. Another option

is to use artificial neural networks to infer the outage size and subsequent optimum load shed amount [7].

All these methods try to minimize the UFLS used post-event, as a containment measure in a system with set FS and commitment decisions. Accurate nadir predictions will implicitly consider system inertia and FR, but offer no framework to compare their cost effectiveness in securing a given outage against UFLS.

In the frequency constrained scheduling literature, the main mathematical challenge lies in containing the frequency nadir, as it necessitates incorporating the dynamic equations dictating post-event frequency evolution into the algebraic optimisation problem [8]. A highly non-linear nadir constraint considering thermal-plant response only, is derived in [9] and implemented in the UC via piece wise linear functions. Reference [10] augments the formulation of [9] to consider response from batteries by suggesting a control scheme that effectively reduces the size of the loss. Reference [11] derives a nadir constraint incorporating response from grid forming inverters which is used in dynamic simulations to determine the set of secure post-outage plant combinations. Appropriate decision variable are then bounded within the UC to insure commitment lies within this set.

References [1], [12]–[14] approximate the FR provision from droop control as a linear ramp to simplify the analytical formulation. These works propose: a linear constraint on FR from turbines in a system with fixed inertia [12]; a linear approximation of the true constraint for systems with variable inertia and single speed FR [1]; and a reformulation of the nadir constraint as a second order cone (SOC), resulting in a SOCP that optimises over inertia, a reduces largest loss, fast and slow FR [13]. All these papers contain the nadir in order to prevent the triggering of UFLS.

The only framework that considers UFLS as an option to contain secured events is [14], whose nadir constraint bounds the product of the FR and inertia from thermal plants to be larger than a constant. The outage size is assumed constant, and the UFLS amount is discretized into blocks, with one nadir constraint per block. The optimizer can then choose the optimal UFLS level to schedule using binary variables. A piecewise linear approximation is used to apply this constraint within a MILP framework.

This paper derives a nadir constraint that allows moderate amounts of UFLS to assist in containing the nadir. Breaking the paradigm of UFLS as a last resort only and demonstrating that when considered alongside other FS, UFLS is a valuable resource to contain outages of the single largest power infeed (credible/secured events) in low inertia systems. The formulation proposed here is significantly more advanced than [14], because it can consider a dynamically reduced largest loss, and multiple speed FR. Both of which [13] has shown to be extremely effective frequency containment measures in low inertia systems, thus vital to consider when accurately evaluating UFLS's value in reducing system FSC. We demonstrate that the proposed nadir constraint can be closely approximated by a single second order cone at each UFLS level. Resulting in a tractable MISOCP formulation that fully exploits the capabilities of modern convex optimisation

solvers.

The key contributions of this work are:

- 1) A comprehensive framework to co-optimise, for the first time, UFLS along with fast and slow FR, inertia and reduced largest loss, to secure frequency in the most cost effective manner.
- 2) A novel, least conservative convexification of the frequency nadir constraint using Second-Order Cones. The computational tractability of this formulation is demonstrated.
- 3) A quantification of the value of UFLS in system operation, considering several sensitivities. Probabilistic scheduling of UFLS is shown to be highly effective for low-inertia power systems.

This paper is organised as follows: Section II details the stochastic unit commitment (SUC) model used to identify the value of UFLS in annual system operation. Section III details the formulation of the convex frequency security constraints and section IV confirms their veracity with dynamic simulations. Case studies exploring the value of UFLS are presented in Section V, whilst section VI gives the conclusion.

## II. STOCHASTIC UNIT COMMITMENT MODEL

This paper applies novel frequency security constraints to a multi-stage unit commitment problem to demonstrate the constraints' value in reducing operating costs. The model optimally schedules energy production, reserve and ancillary services in light of uncertain renewable output.

To capture the critical information about uncertainties, user defined quantiles of the random variable, net demand (demand subtract wind power), are used to construct a scenario tree. The scenarios discretize the continuous range of potential future realisations of the uncertain variable in a representative manner. Reference [15] demonstrates that a small number of well selected scenarios, branching at the root node only, can capture most of the benefit of SUC, with high computational tractability.

The model utilises a rolling planning approach. The operating decisions that minimise the expected cost over the 24hr time horizon are found by using the probability of reaching each scenario as a weighting. It is uneconomical to ensure that for all eventualities demand will be met, so load shedding is permitted in extreme cases. Note,  $P^{LS}$  is load shedding from a lack of reserve, and is distinct from  $P^{UFLS}$  which is load shedding to assist frequency security, which incurs a cost only when it is activated after a generation outage.

The SUC objective function is:

$$\sum_n^N \pi(n) \left( \sum_g^G C_g(n) + \Delta\tau(n) \cdot c_{LS} P^{LS}(n) + C^U(n) \right) \quad (1)$$

The objective function (1) is subject to: generator and storage constraints; the power balance constraint and the frequency security constraints listed in section III. The exhaustive list is found in [15].

The simulation implements the optimal decisions at the here-and-now root node, updating the system states accordingly. At the next time step the actual wind realisation becomes

available, from which a new scenario tree is constructed and the process iterated.

### III. FREQUENCY SECURITY CONSTRAINTS

Each node in the scenario tree has a complete set of system decision variables, so the index  $n$  is dropped in this section to improve equation clarity. After a generator loss, a system's frequency time-evolution is described by the swing equation [16]:

$$\frac{2H}{f_0} \frac{\delta \Delta f}{\delta t} = R_1(t) + R_2(t) - PL_{max} \quad (2)$$

Equation (2) neglects load damping because the level will be significantly reduced in future power-electronic dominated systems [12]. As in [1], [12]–[14], frequency response is modelled as a linear ramp, fully specified by its magnitude and delivery time.

$$R_i(t) = \begin{cases} \frac{R_i}{T_i} \cdot t & t \leq T_i \\ R_i & t > T_i \end{cases} \quad i \in 1, 2 \quad (3)$$

In this paper  $T_1 < T_2$ . The faster speed can correspond to response from power-electronics devices like batteries, while the slower speed is used to model generator dynamics.

The maximum RoCoF occurs the instant of generator disconnection, before any FR has been delivered. The maximum RoCoF must be constrained to prevent distributed generation disconnection (which would further exacerbate the imbalance), derived directly from (2):

$$|RoCoF_{t=0}| = \frac{PL_{max} \cdot f_0}{2H} \leq RoCoF_{max} \quad (4)$$

#### A. Nadir Constraint with UFLS

As shown in (2) frequency decline occurs when demand is larger than generation. From this it follows that the lowest frequency (nadir) will occur at the instant when the power deficit is made zero. Scheduling at least enough FR to cover  $PL_{max}$  insures this will happen before  $T_2$ :

$$PL_{max} < R_1 + R_2 \quad (5)$$

FR reduces the deficit via power injection from storage or generators. UFLS reduces the deficit via a step demand reduction, initiated when low frequency relays measure the local frequency to have dropped below a predefined threshold [17]. As such, in real terms scheduling UFLS simply means scheduling a reduced combination of other FS that allows the frequency to drop below the threshold frequency. The magnitude of demand disconnected is a predetermined discrete block of size  $P^{UFLS}$ . The formulation here allows the system

operator to schedule a range of block magnitudes, achievable when relay settings can be updated hourly. The method to choose between varying UFLS amounts is detailed in section III-C.

The nadir will occur at the UFLS trigger level if the sum of FR delivered by that time and the load shed amount are larger than the outage:

$$P^{UFLS} \geq PL_{max} - R_1 - \frac{R_2}{T_2} \cdot \hat{t} \quad (6)$$

Where  $\hat{t}$  is the time after outage that  $\Delta f(t) = -\Delta f_{trig}$ . Equation (6) assumes that  $\hat{t}$  occurs within the time interval  $T_1 : T_2$ . A valid assumption because equation (5) insures the nadir will always occur before  $T_2$ . The extremely low inertia required for a system to reach  $-\Delta f_{trig} \approx -0.8\text{Hz}$  before  $T_1 \approx 1\text{s}$  would violate (4) for realistic power system parameters.

An expression for  $\hat{t}$  can be found from (2). First, integrate between 0 and  $\hat{t}$  to remove the time derivative:

$$\frac{2H}{f_0} \cdot \Delta f(t) = \frac{R_2}{2T_2} \cdot t^2 - (PL_{max} - R_1) \cdot t - \frac{R_1 T_1}{2} \quad (7)$$

By rearranging and completing the square,  $t$  for a given frequency can be found. Thus the time of  $\Delta f(t) = -\Delta f_{trig}$  is given by (8).

By substituting (8) into (6), the nadir constraint can be formulated:

$$\left( \underbrace{\frac{H}{f_0} - \frac{R_1 \cdot T_1}{4\Delta f_{max}}}_{=z} \right) \underbrace{\frac{R_2}{T_2}}_{=x} \geq \left( \underbrace{\frac{PL_{max} - R_1}{2\sqrt{\Delta f_{trig}}}}_{=y} \right)^2 - \left( \underbrace{\frac{P^{UFLS}}{2\sqrt{\Delta f_{trig}}}}_{=u} \right)^2 \quad (9)$$

Where  $x, y, z$  are linear expressions of decision variables and  $u$  is a constant. Finally, it is useful to rearrange (9) into (10) with the following substitutions:

$$Z = \frac{1}{\sqrt{2}}(x + z), \quad X = \frac{1}{\sqrt{2}}(x - z), \quad Y = y \quad (11)$$

#### B. Nadir Constraint Convexification

The system frequency will not deviate below  $-\Delta f_{trig}$  when constraint (10) is respected. However, it is non-convex so has limited uses in scheduling and market problems due to low tractability and lack of strong duality properties. The convexification proposed here, stems from the observation that (10) is a convex SOC of the classic form  $Z^2 \geq X^2 + Y^2$  when there is no UFLS ( $u = 0$ ). Fig. 1 shows the constraint over a range of  $P^{UFLS}$  values. A 2D plot of the 3D constraint is appropriate because it is symmetrical about any plane that

$$\hat{t} = \frac{T_2}{R_2} \cdot \left( \sqrt{\frac{-4H\Delta f_{trig}R_2 + f_0R_1R_2T_1}{f_0T_2}} + (PL_{max} - R_1)^2 + (PL_{max} - R_1) \right) \quad (8)$$

$$\left( \underbrace{\frac{1}{\sqrt{2}} \left( \frac{R_2}{2T_2} + \frac{H}{f_0} - \frac{R_1 T_1}{4\Delta f_{trig}} \right)}_{=Z} \right)^2 \geq \left( \underbrace{\frac{1}{\sqrt{2}} \left( \frac{R_2}{2T_2} - \frac{H}{f_0} + \frac{R_1 T_1}{4\Delta f_{trig}} \right)}_{=X} \right)^2 + \left( \underbrace{\frac{PL_{max} - R_1}{2\sqrt{\Delta f_{trig}}}}_{=Y} \right)^2 - \left( \underbrace{\frac{P^{UFLS}}{2\sqrt{\Delta f_{trig}}}}_{=u} \right)^2 \quad (10)$$

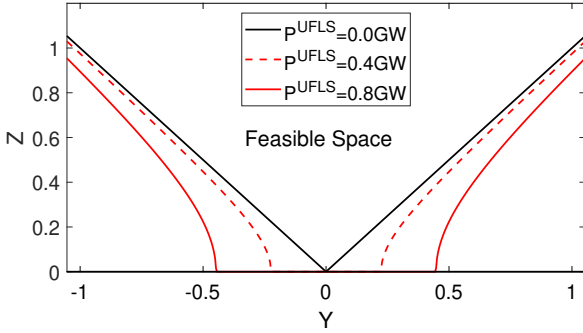


Fig. 1. Feasible space defined by the nadir constraint (10) for various scheduled amounts of UFLS.  $Y$  can be considered as an adjusted outage size and  $Z$  as an adjusted sum of inertia and FR.

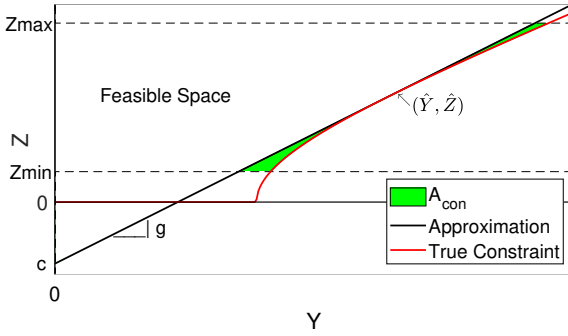


Fig. 2. Convexification of the nadir constraint (10) using a second order cone (16). For a fixed UFLS amount, the SOC's gradient ( $g$ ) and  $Z$  intercept ( $c$ ) are defined by the tangential point  $(\hat{Y}, \hat{Z})$ . The SOC approximation with the minimum  $A_{con}$  is the least conservative.

contains the origin and whose normal is perpendicular to the  $Z$  axis (including  $X = 0$ ).

By considering  $Y$  as an adjusted outage size and  $Z$  as an adjusted sum of inertia and FR, an intuitive understanding of the constraint's function can be found. As the outage size increases, more FR and inertia is needed to contain the frequency above  $(f_0 - \Delta f_{trig})$  Hz. UFLS effectively reduces the outage size, thus diminishing FR and inertia requirements and expanding the feasible space.

Although UFLS makes the feasible space nonconvex, the constraint remains similar to a convex SOC, and indeed tends towards the  $u = 0$  SOC as  $Y$  increases, because  $Y^2 - u^2 \approx Y^2$  when  $Y \gg u$ . Due to this asymptotic behaviour, any SOC tangential to the nonconvex constraint will never intersect it. Thus the SOC will approximate the true feasible space in a convex and conservative manner, as shown in Fig. 2.

The least conservative approximation is best as it enables closer to optimal solutions. For a given  $P_{UFLS}$  this is found by minimising the area between the true constraint and the approximation, labelled  $A_{con}$  in Fig. 2. We are interested in minimising the reduction in feasible space only, thus  $A_{con}$  is further bounded by  $Z_{min}, Z^{max}$  planes. The  $Z$  limits are found by considering the upper and lower bounds of  $R_1, R_2, H$ . These come from (4) and the system specific limits on the provision of these FS from plant and battery levels.

Each point on the constraint's surface has only one pair of SOC gradient ( $g$ ) and zero offset ( $c$ ) that gives the tangential SOC. Thus due to the symmetry about the origin, these are functions of  $Z$ .  $g$  is the gradient of the constraint (10) at the  $Z$  value of interest ( $\hat{Z}$ ):

$$\hat{Y}(\hat{Z}) = \sqrt{\hat{Z}^2 + u^2} \quad (12)$$

$$g(\hat{Z}) = \frac{\delta Z}{\delta Y}(\hat{Y}(\hat{Z})) = \frac{\hat{Y}}{\sqrt{\hat{Y}^2 - u^2}} \quad (13)$$

Then  $c$  is found as the value that a line with gradient  $g$  passing through  $(\hat{Y}, \hat{Z})$  crosses the  $Z$  axis:

$$c(\hat{Z}) = \hat{Z} - g(\hat{Z}) \cdot \hat{Y} \quad (14)$$

The  $g$  and  $c$  that minimise the area  $A_{con}(g, c)$  (labelled here as  $(g_{opt}, c_{opt})$ ) result in the least conservative SOC approximation because they reduce the feasible space the least. These are found offline by searching over the feasible  $\hat{Z}$  range ( $Z_{min} : Z^{max}$ ). Thus the new convex, least conservative SOC nadir constraint is given by:

$$Z \geq g_{opt} \sqrt{X^2 + Y^2} + c_{opt} \quad (15)$$

$$\frac{1}{g_{opt}}(Z - c_{opt}) \geq \sqrt{X^2 + Y^2} \quad (16)$$

### C. Optimising UFLS amount

A constant  $P_{UFLS}$  facilitates the convexification, but to optimally balance the UFLS as an option against other FS, an optimizer must be able to choose the amount of UFLS to schedule. Binary variables enable this by successively relaxing any nadir constraint with less UFLS, successively increasing the feasible space and the expected UFLS cost. Assuming:

$$P_1^{UFLS} < P_2^{UFLS} < \dots < P_N^{UFLS} \quad (17)$$

Then the Big M technique can be implemented with (16) to allow UFLS level choice:

$$Z + M(m_1 + m_2 + \dots + m_K) \geq \sqrt{X^2 + Y^2} \quad (18a)$$

$$\frac{1}{g_{opt}(P_1^{UFLS})}(Z - c_{opt}(P_1^{UFLS})) + M(m_2 + \dots + m_K) \geq \sqrt{X^2 + Y^2} \quad (18b)$$

...

$$\frac{1}{g_{opt}(P_{K-1}^{UFLS})}(Z - c_{opt}(P_{K-1}^{UFLS})) + M \cdot m_K \geq \sqrt{X^2 + Y^2} \quad (18c)$$

$$\frac{1}{g_{opt}(P_K^{UFLS})}(Z - c_{opt}(P_K^{UFLS})) \geq \sqrt{X^2 + Y^2} \quad (18d)$$

$$m_1 + m_2 + \dots + m_K \leq 1 \quad (19)$$

The above formulation is a convex SOC because the left hand side remains a linear expression of decision variables. Thus the nadir constraint (18) can be efficiently solved by any convex solver with MISOCP capabilities, facilitating its tractable application to a wide range of scheduling and market problems. To reduce solver times, it is recommended to keep

$M$  as small as possible and to add the binary variables  $m_k$  at each node to a special ordered set.

If  $P^{UFLS}$  is scheduled when a  $PL_{max}$  outage occurs, then that amount of demand will be disconnected. The cost depends on the value of the load that is disconnected ( $c^{UFLS}$ ) and the disconnection length. However, despite being costly when it is utilised, large outages occur rarely so UFLS is seldom triggered, but can substantially reduce the requirements on the other frequency services. To explore this balance, the expected cost of UFLS is added to the cost function, and included in the FSC:

$$C^U = t_{rec} \cdot p \cdot N_{PL_{max}} \left( \sum_{k=1}^K m_k \cdot c_k^{UFLS} \cdot P_k^{UFLS} \right) \quad (20)$$

Finally, (20) does not accurately characterise the expected cost of UFLS if any losses smaller than  $PL_{max}$  would trigger the demand disconnection. This can be prevented by implementing an additional constraint equivalent to (10) at each node, with  $P^{UFLS} = 0$  and  $PL_{max}$  equal to the next largest system outage. This guarantees that UFLS would only be activated for the largest credible contingency.

#### IV. CONSTRAINT VERIFICATION

This section uses dynamic simulations to verify that the nadir constraint (18) does contain the system frequency, whilst also offering insight into how the different FS interact to do so. Figure 3 plots  $\Delta f(t)$  following a  $PL_{max}$  outage for the system conditions described in Table I, all of which lie on (18). The FR time constants are  $T_1 = 1s$ ,  $T_2 = 10s$ . The nadir will always coincide with the trigger level, because constraint (18) guarantees that the triggered UFLS is sufficient to close the generation-demand deficit, arresting frequency drop.

No UFLS is scheduled in cases A and B. Consequently, there is just enough FR and H in both cases to insure that the frequency reaches, but does not cross the UFLS trigger level. However, to secure a loss only 0.2 GW smaller than case B, case A needs 39.1 GWs less inertia. This is equivalent to the inertia from approximately 20 combined cycle gas turbines (CCGTs). Similarly, comparison between cases C and D shows that fast FR is also an effective FS, with a 0.1 GW difference reducing inertia requirement by 18.6 GWs ( $\approx 9$  CCGTs).

Case C has 20.9 GWs ( $\approx 10$  CCGTs) less inertia than case B. This reduction means that the system frequency breaches the trigger level and UFLS is initiated. The step change in demand reverts the frequency gradient to zero, thus the trigger level corresponds to the nadir. In other words, UFLS has reduced the system's inertia requirements at the expense of an increased UFLS expected cost (20). The constraints developed in this paper offers the optimiser a tool to find the optimal balance between these competing effects during scheduling.

#### V. CASE STUDIES

The SUC model was used to identify the savings in FSCs from UFLS. Each simulation corresponds to four months operation of a representative GB 2030 system, one from each season. A scenario tree branching 7 times at the root node only was used to account for net demand forecast uncertainty,

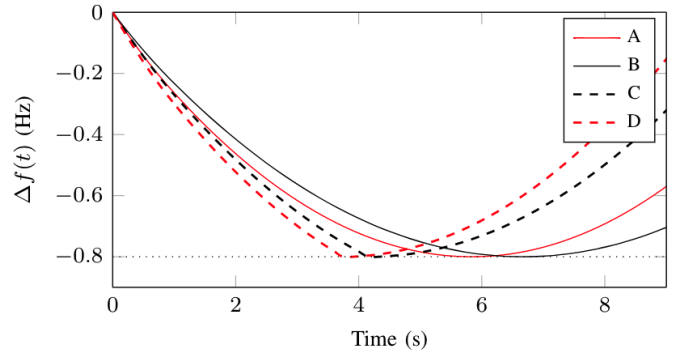


Fig. 3. Frequency evolution after a loss of  $PL_{max}$  for the system conditions in Table I.

TABLE I  
DYNAMIC SIMULATION PARAMETERS

|   | $P^{UFLS}$ (GW) | $R_1$ (GW) | $R_2$ (GW) | $H$ (GWs) | $PL_{max}$ (GW) |
|---|-----------------|------------|------------|-----------|-----------------|
| A | 0.0             | 0.2        | 2.4        | 130.7     | 1.6             |
| B | 0.0             | 0.2        | 2.4        | 169.8     | 1.8             |
| C | 0.6             | 0.2        | 2.4        | 146.3     | 1.8             |
| D | 0.6             | 0.3        | 2.4        | 127.7     | 1.8             |

as detailed in [15], with quantiles of 0.005, 0.1, 0.3, 0.5, 0.7, 0.9 and 0.995.

A typical time-series of demand was used, with a range of 20:60 GW with daily and seasonal trends. Unless otherwise stated there is an installed wind capacity of 35 GW, and a storage and generation mix detailed in Table II. Frequency security requirements were aligned with GB standard,  $RoCoF_{max} = 1$  Hz/s and  $|\Delta f_{max}| = 0.8$  Hz. The FR time constants are  $T_1 = 1s$ ,  $T_2 = 10s$ , while  $c_{LS} = \text{£}30,000/\text{MWh}$  and  $c^{UFLS} = \text{£}30,000/\text{MWh}$  unless otherwise stated. UFLS was assumed to disconnect load for 1h when utilised, implying that a system re-dispatch would be possible within one hour of the outage.  $PL_{max}$  is determined by the power output of nuclear plants, which have an assumed outage rate of 1.8 occurrences/yr.

Simulations were run in an 8 core Intel Xeon 2.40GHz CPU with 64GB of RAM. XPRESS 8.10 was used to solve the optimisations linked to a C++ application via the BCL interface. The MISOCP duality gap was 0.1%.

##### A. Evaluation of the Conservativeness of Nadir Constraint Approximation

Equation (18) conservatively approximates the true non convex feasible space. This produces a highly tractable MISOCP formulation that guarantees system security, at the cost of a reduced feasible space potentially decreasing a solution's optimality. In operational terms, this translates into the over-scheduling of FS. The severity is measured by calculating the minimum nadir that the scheduled FS could secure ( $\Delta f_{trig}^{true}$ ). The closer this value is to  $\Delta f_{trig}$ , the more optimal the solution, and the better the approximation. The nadir constraint with 0 GW UFLS is not an approximation, so it is not conservative.

Figure 4 shows the distribution of  $\Delta f_{trig}^{true}$  for simulations where 2 UFLS levels are available, 0 GW or the value

TABLE II  
GENERATION AND STORAGE CHARACTERISTICS

| Generation                 | Nuclear | CCGT      | OCGT      |
|----------------------------|---------|-----------|-----------|
| Number of Units            | 4       | 120       | 20        |
| Rated Power (GW)           | 1.8     | 0.5       | 0.1       |
| Min Stable Generation (GW) | 1.60    | 0.25      | 0.05      |
| No-Load Cost (£'000/h)     | 0.0     | 4.5       | 3.0       |
| Marginal Cost (£/MWh)      | 10      | 47        | 200       |
| Startup Cost (£'000)       | NA      | 10        | 0         |
| Startup Time (h)           | NA      | 3         | 0         |
| Min up Time (h)            | NA      | 4         | 0         |
| Inertia Constant (s)       | 5       | 4         | 4         |
| Max R2 Capacity (GW)       | 0.00    | 0.05      | 0.05      |
| Storage                    | Pumped  | Battery 1 | Battery 2 |
| Capacity (GWh)             | 10      | 1         | 12        |
| Dis/Charge Rate (GW)       | 2.6     | 0.3       | 3.0       |
| Max R1 Capacity (GW)       | 0.0     | 0.6       | 0.0       |
| Max R2 Capacity (GW)       | 0.5     | 0.0       | 0.0       |
| Dis/Charge Efficiency      | 0.75    | 0.95      | 0.95      |

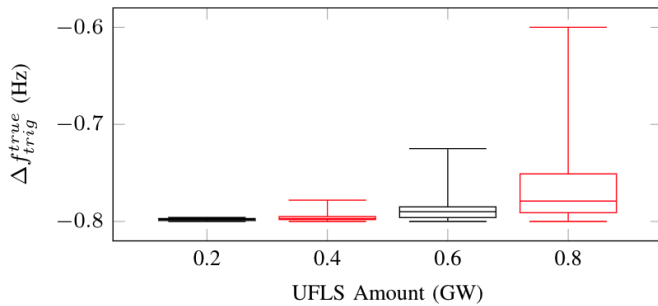


Fig. 4. The conservative approximation of (10) by (18) results in the over scheduling of FS, which could secure a stricter nadir ( $\Delta f_{true}^{true}$ ) than that required ( $\Delta f_{true}^{true} = 0.8$  Hz). Shown here are the annual inter-quartile range, median and max/min of  $\Delta f_{true}$  for systems with two levels of UFLS available, 0 GW or the value shown on the x axis.

shown on the x axis. For  $P_{UFLS}^{UFLS} = 0.6$  GW, the median  $\Delta f_{max}^{true} = -0.79$  Hz, and the most conservative is -0.73 Hz. Demonstrating that for this level of load shed, the formulation gives solutions that are always less than 10% conservative, with the vast majority being significantly less so.

The clear trend of increasing conservativeness with  $P_{UFLS}^{UFLS}$  in Fig. 4 can be explained by Fig. 1. Larger UFLS levels increase the curvature of the nadir constraint, thus approximating it with a straight line is less accurate. In other words, the minimum area of  $A_{con}(g, c)$  becomes larger and the approximation more conservative. However, over the realistic range of available UFLS studied here, the constraint is at the worst 25% conservative when  $P_{UFLS}^{UFLS} = 0.8$  GW. Even so, when  $P_{UFLS}^{UFLS} = 0.8$  GW the true nadir was below -0.7 Hz over 95% of the time. Thus most solutions are very close to optimal and insight into the value of UFLS is unhindered. Larger amounts of UFLS are not considered here to avoid activating the nadir constraints for losses smaller than N-1.

### B. Value of UFLS in reducing FSC

Fig. 5 shows reduction in annual FSC when two levels of UFLS are available, 0 GW or the value shown on the x axis. The FSC for a system with no UFLS is £1072 m/yr, 10.8% of total system costs. Allowing 0.8 GW of UFLS offers

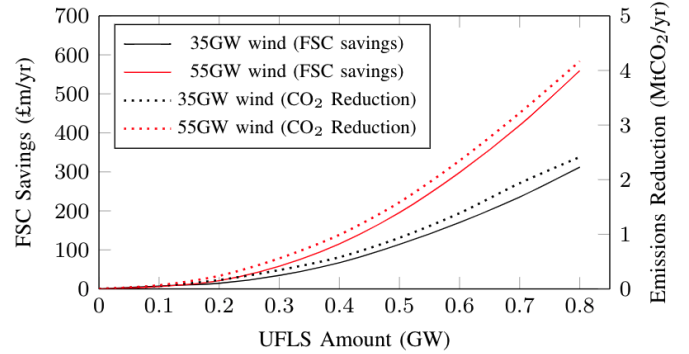


Fig. 5. The annual reduction in frequency security costs and emissions from optimally scheduling UFLS to support frequency security, in systems with 35 GW and 55 GW of installed wind capacity.

a 52% reduction of £559m/yr, and 0.4 GW by £115m/yr. These reductions include the increase in expected cost of outages from allowing UFLS, and demonstrate that UFLS can significantly improve system operation in systems with high renewable penetration.

The UFLS creates value by reducing the FS required from thermal plants whose minimum generation drives wind curtailment during low net demand periods. An example of this phenomenon is shown in Figure 6, which compares the optimal commitment of CCGT plants over the same 3-day period for two identical systems. One has the option to schedule 0.6 GW of UFLS and the other does not. CCGTs are shown because nuclear plants have a fixed commitment and the OCGT output is negligible over the depicted period. During the high net demand period on the first day, no UFLS is scheduled because frequency security requirements are met as a by-product of energy supply. Accordingly, both systems have similar plants commitment levels.

Overnight, the demand drops and wind output increases, staying high for the following days. Over this period, the scheduled UFLS makes containing the frequency possible whilst needing less inertia and FR from the thermal plants, so fewer CCGTs are run. This lowers the sum of their minimum generation, enabling the absorption of up to 4.7 GWh more wind energy per hour. UFLS's ability to facilitate the absorption of more zero marginal emission wind energy explains the CO2 savings in Fig. 5. Furthermore, when there is higher installed wind generation capacity low net demand periods are more frequent, thus FSC and emission savings increase.

### C. Value's Dependence on the Availability of Fast FR and a Reduced Largest Loss

Figure 7 shows the reduction in FSC from the optimal scheduling of 0.6 GW of UFLS, in systems with varying availability of other FS. The (dis)charge rate of Battery 1 in Table II was adjusted to simulate varying  $R_1$  capacities. The minimum stable generation of nuclear plants was varied to change the lower bound of  $PL_{max}$ .

To accurately evaluate UFLS, explicit consideration of the available  $PL_{max}$  reduction and  $R_1$  is vital. It was shown in

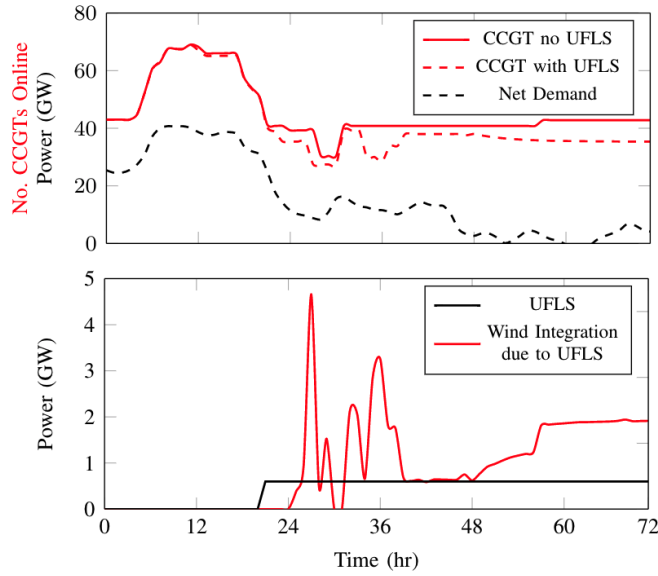


Fig. 6. Three-day example of the system operation, showcasing the use of UFLS to accommodate more wind.

section IV that these two FS are highly effective at arresting frequency decline, so they compete with UFLS to reduce wind curtailment and create value. Figure 7 shows that as the availability of other FS increases, the value of UFLS decreases from £195m/yr in a system with only UFLS,  $H$  and  $R_2$ , to £80m/yr in a system with abundant  $R_1$  and  $PL_{max}$ . This demonstrates why a framework that considers these two FS is essential when defining the value of UFLS. It also highlights that UFLS remains competitive as a FS even in highly flexible systems, so must be considered when operating future high RES systems efficiently.

Interestingly, Fig. 7 shows that when  $PL_{max} = 1.8\text{GW}$ , the value of UFLS is approximately constant with increasing  $R_1$  availability. This is because the nadir requirements at this large loss level cause extreme levels of wind curtailment. There is 28.6 GWh of annual wind curtailment with no UFLS or  $R_1$ , corresponding to a FSC of £2.23bn/yr, which is 25% of total system costs. When FSC is this high, additional  $R_1$  and UFLS can simultaneously reduce it, without infringing on the other service's marginal value. This compares to the lowest FSC cost of £0.37bn/yr, 4% of the operating cost of the system with  $R_1 \leq 1.2\text{GW}$ ,  $PL_{max} \geq 1.4\text{GW}$ ,  $UFLS = 0.6\text{GW}$ .

#### D. Impact of the Expected Cost of UFLS

According to [18] the value of load-shed in the UK ranges between 2:45 £'000/MWh depending on the consumer type, importance, season and time of day. In reality it is likely that lower cost loads would be disconnected to support frequency security, so the assumption of  $c^{UFLS} = £30,000/\text{MWh}$  used so far in this paper is a conservative one. Figure 8 details the sensitivity of UFLS value to  $c^{UFLS}$  in 3 separate cases: 'Free UFLS' when  $c^{UFLS} = 0$ ; 'Fixed UFLS' when UFLS is scheduled at all times; 'Optimal UFLS' when the optimiser can choose when to schedule UFLS.

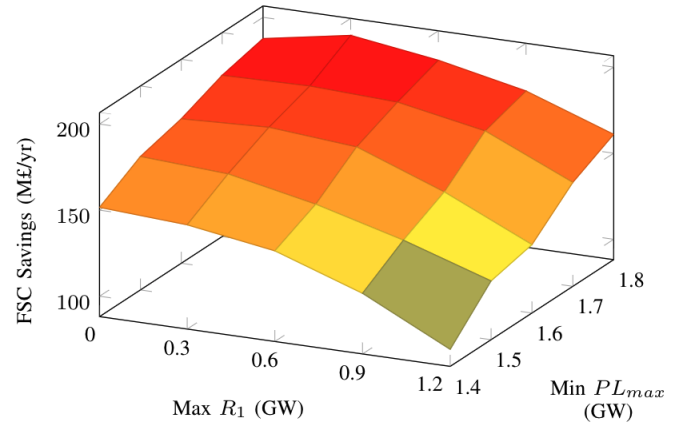


Fig. 7. Savings in annual frequency security costs enabled by 0.6 GW of UFLS in systems with different amounts of fast FR ( $T=1\text{s}$ ) and different capabilities to dynamically lower the maximum outage size.

As the expected cost decreases, the penalty for scheduling UFLS decreases, so it is scheduled more frequently and the FSC savings increase. For example, if  $c^{UFLS}$  is halved to £15,000/MWh, then Fig. 8 shows that the FSC savings from UFLS increase by £41m/yr.

The expected cost of UFLS ( $C^U$ ) is the product of the probability that an outage will occur and the cost of load shedding if it does. As shown in (20),  $C^U$  is linearly dependant on  $c^{UFLS}$ , as well as  $t_{rec}, p, N_{Gmax}$ . So the sensitivity results in Fig. 8 are applicable to adjusting those values also. In other words, if the nuclear plants outed half as often, or the demand was disconnected for half as long, savings of £41m/yr would be observed as those changes are equivalent to reducing the cost of load shedding from £30,000/MWh to £15,000/MWh.

The 'Free UFLS' value in Fig. 8 corresponds to a system with a permanently reduced FS requirement. As such it represents the maximum FSC reduction from UFLS possible, and is trended towards as  $c^{UFLS}$  decreases. On the other hand, as  $c^{UFLS}$  increases the 'Optimal UFLS' value trends towards 0 because the larger cost of outage makes UFLS a less attractive option to contain the frequency. Above  $c^{UFLS} = £60,000/\text{MWh}$  'Fixed UFLS' shows that always scheduling UFLS begins to increase system costs. This is because the gains from reduced FS requirements, facilitating higher wind absorption, are entirely offset by the severe cost when an outage occurs. The difference between 'Fixed UFLS' and 'Optimal UFLS' is the value in allowing the optimiser to choose via binary variables (18), to secure the nadir with UFLS or not.

#### E. Impact of an Increasing Marginal Load-Shed Cost

Comparison between case  $\alpha$  and  $\beta$  in Table III shows the impact of discretising the UFLS into smaller steps. The options to schedule 0.2 GW and 0.4 GW alongside 0 GW and 0.6 GW are introduced. This produces no FSC savings, while computation time increased by 68%. This is because  $P^{UFLS}$  has increasing marginal gains, due to its quadratic factor in (10), but only linearly increasing costs (20). Accordingly, it is optimal to schedule UFLS levels smaller than 0.6 GW,

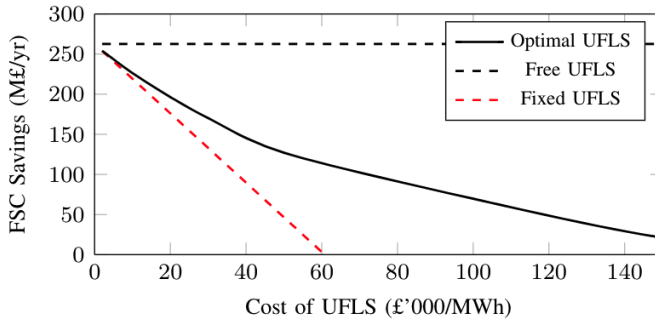


Fig. 8. Sensitivity of frequency security savings from 0.6 GW of UFLS to the cost of the load shed ( $c_{UFLS}$ ): ‘Free UFLS’ load shed is zero cost; ‘Fixed UFLS’ UFLS is scheduled at all times; ‘Optimal UFLS’ optimiser chooses when to schedule UFLS.

TABLE III  
IMPACT OF A VARIABLE MARGINAL UFLS COST

|          | UFLS Steps (GW)    | Marginal UFLS Cost (£'000/MWh) | Time at UFLS level (%) |
|----------|--------------------|--------------------------------|------------------------|
| $\alpha$ | 0.0, 0.6           | 30                             | 49.3, 50.7             |
| $\beta$  | 0.0, 0.2, 0.4, 0.6 | 30, 30, 30                     | 50.2, 0.5, 0.3, 49.0   |
| $\gamma$ | 0.0, 0.2, 0.4, 0.6 | 1, 10, 79                      | 21.0, 0.2, 48.9, 29.9  |
|          | FSC (£m/yr)        | Run Time (h)                   |                        |
| $\alpha$ | 907.8              | 5.7                            |                        |
| $\beta$  | 907.8              | 9.6                            |                        |
| $\gamma$ | 897.2              | 7.2                            |                        |

less than 1% of the year. This justifies the preceding case studies only considering one UFLS level other than 0 GW. This phenomenon also explains the quadratic increase in FSC savings depicted in Fig. 5.

However, in reality the marginal  $c_{UFLS}$  often increases due to load being shed in the order of value. The formulation can account for this. For case  $\gamma$  in table III, the first 0.2 GW of scheduled load shed costs only £1,000/MWh, the second 0.2 GW costs £10,000/MWh and the final costs £79,000/MWh. In this case it is optimal to schedule 0.4 GW of UFLS for 48.9% of the year, a dramatic increase compared to case  $\beta$ . Explicitly recognising this cost variation facilitates a more optimal system operation, resulting in an annual FSC reduction of £10.6m, despite the fact that the average cost of loadshed is £30,000/MWh when 0.6GW of UFLS is scheduled for both cases  $\beta$  and  $\gamma$ .

## VI. CONCLUSION

This paper analytically derives a constraint on the frequency nadir from the swing equation. This constraint insures that there is sufficient fast and slow FR, inertia and UFLS scheduled to contain the largest system loss, which itself can be dynamically reduced to improve operation. We show that when the UFLS amount is discretized, the nonconvex constraint can be accurately and conservatively approximated by a convex second order cone. Case studies were run to explore how scheduled UFLS translates into a reduced requirement on other FS, translating into significantly enhanced integration of wind energy due to the lower response requirements from thermal plants. We demonstrate that drastic cost reductions are achievable by breaking the current paradigm of UFLS as a last

resort containment measure. Furthermore the constraint offers insight into the synergies and conflicts between the diverse FS considered. A key take away is that UFLS remains valuable even in highly flexible systems.

There are two main ways to enhance the model in future work. Firstly, this paper focuses purely on how to operate a system at least cost. Availability and utilisation payments for the different FS are not considered. As such, considering UFLS as a service within a market context would allow the investigation of pricing schemes that reflect the appropriate value of different services. Secondly, this paper only considers how UFLS can assist with frequency containment after the loss of the single largest plant. UFLS for unsecured events is considered separate. This framework could enable efficiency gains by blurring this distinction, facilitating a holistic method to schedule UFLS across all possible events in light of the available FS.

## REFERENCES

- [1] F. Teng *et al.*, “Stochastic Scheduling with Inertia-Dependent Fast Frequency Response Requirements,” *IEEE Transactions on Power Systems*, vol. 31, no. 2, pp. 1557–1566, mar 2016.
- [2] “National Electricity Transmission System Security and Quality of Supply Standard,” The SQSS Review Panel, Tech. Rep. v2.4, April 2019.
- [3] H. Haes Alhelou *et al.*, “An Overview of UFLS in Conventional, Modern, and Future Smart Power Systems: Challenges and Opportunities,” *Electric Power Systems Research*, vol. 179, p. 106054, 2020.
- [4] M. Sanaye-Pasand and H. Seyedi, “New centralised adaptive load-shedding algorithms to mitigate power system blackouts,” *IET Generation, Transmission & Distribution*, vol. 3, no. 1, pp. 99–114, jan 2009.
- [5] V. V. Terzija, “Adaptive underfrequency load shedding based on the magnitude of the disturbance estimation,” *IEEE Transactions on Power Systems*, vol. 21, no. 3, pp. 1260–1266, aug 2006.
- [6] U. Rudez and R. Mihalic, “WAMS-Based Underfrequency Load Shedding with Short-Term Frequency Prediction,” *IEEE Transactions on Power Delivery*, vol. 31, no. 4, pp. 1912–1920, aug 2016.
- [7] R. Hooshmand and M. Moazzami, “Optimal design of adaptive under frequency load shedding using artificial neural networks in isolated power system,” *International Journal of Electrical Power and Energy Systems*, vol. 42, no. 1, pp. 220–228, nov 2012.
- [8] J. Luo *et al.*, “Stability-constrained Power System Scheduling: A Review,” *IEEE Access*, 2020.
- [9] H. Ahmadi and H. Ghasemi, “Security-constrained unit commitment with linearized system frequency limit constraints,” *IEEE Transactions on Power Systems*, vol. 29, no. 4, pp. 1536–1545, 2014.
- [10] Y. Wen *et al.*, “Frequency Dynamics Constrained Unit Commitment with Battery Energy Storage,” *IEEE Transactions on Power Systems*, vol. 31, no. 6, pp. 5115–5125, nov 2016.
- [11] M. Paturet *et al.*, “Stochastic unit commitment in low-inertia grids,” *IEEE Transactions on Power Systems*, vol. 35, no. 5, pp. 3448–3458, sep 2020.
- [12] H. Chavez *et al.*, “Governor rate-constrained OPF for primary frequency control adequacy,” *IEEE Transactions on Power Systems*, vol. 29, no. 3, pp. 1473–1480, 2014.
- [13] L. Badesa *et al.*, “Simultaneous Scheduling of Multiple Frequency Services in Stochastic Unit Commitment,” *IEEE Transactions on Power Systems*, vol. 34, no. 5, pp. 3858–3868, sep 2019.
- [14] F. Teng and G. Strbac, “Full Stochastic Scheduling for Low-Carbon Electricity Systems,” *IEEE Transactions on Automation Science and Engineering*, vol. 14, no. 2, pp. 461–470, apr 2017.
- [15] A. Sturt and G. Strbac, “Efficient stochastic scheduling for simulation of wind-integrated power systems,” *IEEE Transactions on Power Systems*, vol. 27, no. 1, pp. 323–334, feb 2012.
- [16] P. Kundur, *Power System Stability and Control*, 1st ed. McGraw-Hill Education, 1994.
- [17] Western Power Distribution, “Low frequency demand disconnection.” Report, June 2017.
- [18] London Economics, “The Value of Lost Load (VoLL) for Electricity in Great Britain: Final report for OFGEM and DECC,” *OFGEM and DECC*, no. July, pp. 1–225, 2013.